探討以紅外線加熱溶膠凝膠法製作摻雜鋁氧化鋅薄膜載子之活化效應

*1林克默、2陳信誠
南台科技大學機械工程系
*1kemo@mail.stut.edu.tw, 2m9710246@gmail.com

摘要

本研究探討紅外線加熱溶膠凝膠法對摻雜鋁氧化鋅薄膜光電與化學性質的影響，文中並討論鋁和鎂的摻雜量對於載子的活化效果。實驗顯示，如同摻雜鎵氧化鋅薄膜一般，紅外線加熱法可有效改變摻雜鋁氧化鋅薄膜的孕核行爲，並明顯提高摻雜鋁氧化鋅薄膜的導電性。而高活性的鎂離子除可改變溶膠錯合物的結構外，並能改變氧化鋅孕核行爲以及載子活化效率。由於添加鎂可降低溶膠內醋酸鋅單體的沉澱速率，因此能稍提高摻雜鋁氧化鋅薄膜的載子濃度。但過量的鎂含量會阻礙載子的運動，並降低載子遷移率，導致薄膜導電率變差。

關鍵詞：載子活化、紅外線加熱、氧化鋅、溶膠凝膠法、透明導電氧化物

Carrier Activation of Sol-gel Derived ZnO:Al Films Using Infrared Heating Method

Keh-Moh Lin, Hsin-Cheng Chen
Department of Mechanical Engineering, Southern Taiwan University

Abstract

The purpose of this paper is to examine how Infrared heating procedure affects the opto-electrical and chemical properties of ZnO:Al (AZO) films and to investigate the influences of Al and Mg elements on the dopant activation of AZO films prepared by sol-gel method. In our experiments, the infrared heating method effectively enhanced the activation effects of Al dopant and thus improved the conductivity of AZO films. Moreover, the electropositive Mg was successfully used to modify the complex structure in the sol solution and to affect the nucleation as well as the carrier activation behaviors of the AZO films. Experimental results show that adding Mg could slightly increase the carrier concentration because it productively constrained the precipitation of zinc monoacetate in the sol-solution and retarded the oxidation of Al during the film growth process. Yet too much Mg lowered the carrier mobility, and the conductivity was thus reduced.

Keywords: Carrier Activation, Infrared Heating, Zinc Oxide, Sol-gel, Transparent Conductive Oxide.

Received: Nov. 28, 2011; accepted: April, 2012.
*Corresponding author: K-M. Lin

I. Introduction

Due to the high material cost of traditional mono- and poly-crystalline silicon solar cells, thin film and other kinds of solar cells have been attracting a lot of attention [1, 2]. The conversion efficiency and life-span of thin film solar cells, whose transparent electrodes are made of transparent conductive oxides (TCO), are directly affected by the electrical performance and durability of the TCO materials. Different from LCDs, whose transparent electrodes are made of Indium Tin Oxide (ITO), the transparent electrodes of thin film solar cells mainly uses SnO_2:F (FTO) or doped ZnO as material. It is well known that ZnO is a low cost, abundant, and nontoxic material. Moreover, the doped ZnO films are well resistant against being reduced to metallic zinc under plasma environment because of its surface protection layer [3]. ZnO:Al (AZO) film has already found its way in the fabrication of transparent electrodes in solar cells [4,5]. Recently, doped ZnO has been successfully deposited as a thin film with low resistivity on substrates with low melting temperatures [6]. However, to apply TCO materials on the transparent electrodes of thin film solar cells, we need to consider various factors, such as the production cost and its compatibility with the following fabrication procedures. The sol–gel method is not only low-cost but also efficient in depositing large area TCO films for technological applications. In addition, the co-doping technique allows us to modify TCO's properties, for it has been successfully applied to overcome the etching problem of doped ZnO films [7].

In this study, we intend to study the feasibility of using a rapid thermal anneal (RTA) processor based on infrared heating technology to improve the electrical properties of AZO films. In addition, we also investigate the possibility of using Mg, a more electropositive element, to modify the complex structure of the sol solution and to retard the oxidization of Al atoms to reach the goal of enhancing the activation process of Al dopant.

II. Coating preparation and characterization

In this study, zinc acetate (ZnAc) was dissolved in ethanol, and aluminum nitrate was served as dopant sources. Monoethanolamine (MEA) was used as stabilizer. The atomic ratio Al/Zn of AZO specimens was between 0.25 ~ 5.0 at.%. To prepare Al and Mg co-doped ZnO (AMZO) films, magnesium acetate (MgAc) was added to make the atomic ratio Mg/Zn to be 0.5 or 1.0 at.% as well as the atomic ratio Al/Zn to be 0.25 ~ 1.0 at.%. Afterwards, AZO and AMZO films were spin-coated on glass substrates (corning 1737). Then, the specimens were heated in a RTA furnace at 600 ºC for 10 min. The post-heat treatment was carried out in a tube furnace in vacuum (150 mtorr) at 600 ºC for 1h. Some AMZO specimens were preheated in a tube furnace (TF) at 600 ºC for 30 min. [8,9].

The crystallinity of the AZO and AMZO films was studied by a thin-film X-ray diffractometry with an incident angle of 1° (Rigaku D/MAX 2500). A field emission scanning electronic microscope (JEOL 7401F) was used to observe the morphology and the microstructures of the cross-section of the doped ZnO films. The thicknesses of the AZO and AMZO films were measured by a UV-Vis-NIR spectrophotometer (Jacos V-670). The electrical properties were first obtained by a Hall measurement system (Ecopia HMS-3000) and then examined by a four-point probe station. The optical properties of these films and the sol solution were obtained by Fourier Transform Infrared Spectrometer (FTIR) (Thermo Nicolet, Nexus) and the UV-Vis-NIR spectrophotometer. The chemical bonding states of the films were studied with an X-ray photoelectron spectroscopy (PHI 5000).

III. Results and discussion

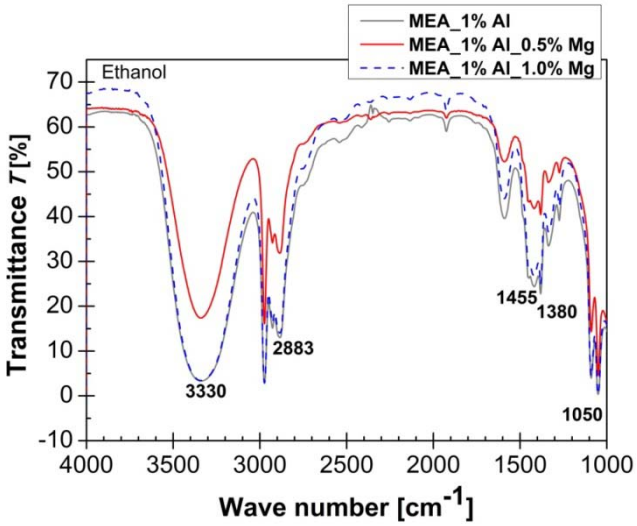

Figure 1 FTIR transmittance spectra of different kinds of precursors. The absorption of O-H bonds at 3330 cm^{-1} became weaker due to adding of MgAc.

1. FTIR Analyses

The FTIR transmittance spectra of the precursors are given in Figure 1. The absorption due to the O-H bond in ethanol solvent is found in the range from 3100 - 3600 cm^{-1}. The peak under 3000 cm^{-1} represents the C-H bonds, and also the troughs between 1000 and 1100 cm^{-1}. One of which will be due to the C-O bond. The possible absorption due to the C-O bond under 1500 cm^{-1} is queried because it lies in the fingerprint region. They showed in Figure 1 that the absorption of O-H bonds at 3330 cm^{-1} became weaker after adding a certain amount of magnesium acetate. The solutions became clearer, indicating that Mg^{2+} ions slowed the hydrolysis process and effectively retarded the precipitation reaction of zinc monoacetate [10].

We then further analyzed the change of the FTIR transmittance spectra after the films underwent heat treatments under different temperatures (Figure 2). The reference curve (a) shows the FTIR transmittance spectrum of the ethanol solvent while curves (b) to (e) are the spectra of the AMZO films (0.5 at.% Mg + 0.75 at.%Al) . In curve (b) we see the spectrum of the AMZO films dried at 50 °C. The peaks at 1577 and 1394 cm^{-1} indicate the existence of C=O bonds [11] while the broad peak in the range 3000 to 3500 cm^{-1} was mainly due to O-H bonds of the ethanol. Curve (c) shows the spectrum of the deposited film dried at 120 °C. The peak in the range 3000 to 3500 cm^{-1} was broader. The peak at 3291 cm^{-1} indicates the present of N-H bonds in the MEA. Because ethanol and acetic acid already evaporated at 120 °C, the O-H and N-H bonds mainly belonged to zinc monoacetate and MEA [11]. When the deposited film was dried at 250 °C (curve d), the broad peak became narrower. At this moment, MEA also evaporated, and most zinc monoacetate was transformed into $Zn(OH)_2$. In addition, the peak at 1577 cm^{-1} disappeared gradually and the peak at 1394 cm^{-1} shifted to 1384 cm^{-1} as annealing temperature increased. The retained peak at 1384 cm^{-1} suggests that these are due to some complicated bending vibrations within the films. Curve (e) indicates after the films were heated under 350 °C, most $Zn(OH)_2$ were transformed into ZnO, which appeared at 500 cm^{-1}. At this moment, there was still a small amount of organic bonds or bending vibrations in the films. Finally, curve (f) shows the FTIR transmittance spectrum of an AZO film, which was similar to that of the curve (c). From these results, we can conclude that adding magnesium acetate mainly constrained the precipitation of zinc monoacetate while the structure of the complexes was not changed.

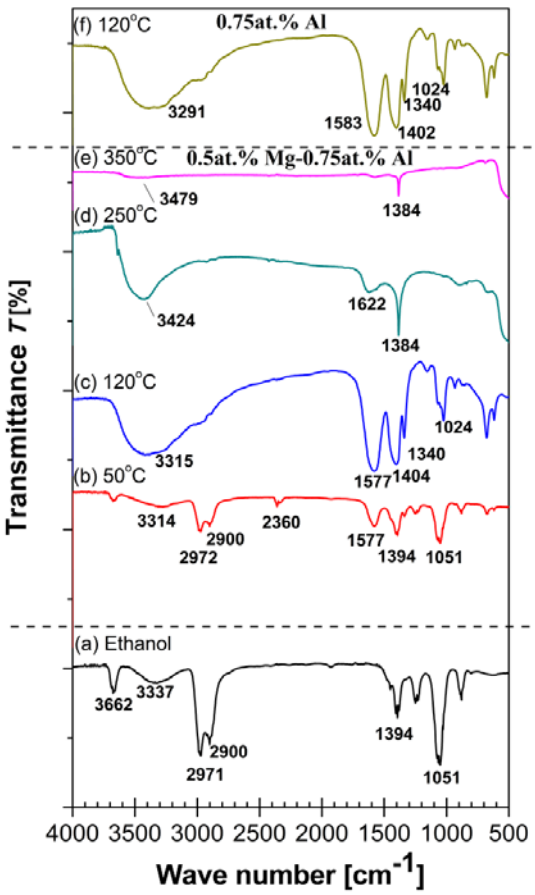

Figure 2 FTIR transmittance spectra after the precursors underwent different heat treatments. (a) precursor, 0.5 at.% Mg, 0.75 at.% Al; (b) dried at 50 °C; (c) dried at 120 °C; (d) dried at 250 °C; (e) dried at 350 °C; (f) precursor, 0.75 at.% Al. Solvent: Ethanol.

2. SEM Observation

Figure 3 is the over-view and cross section of the AMZO films. Unlike the films deposited by the sputter process, these images show granular-structured layers stacking one upon another [9]. So the microstructure was rather loose, suggesting the growth of the films began inside the sol-layer (Figure 3a & 3b).

The SEM pictures of the TF process show that with a certain amount of Mg, the crystallite size became smaller along with the increasing Al amount, so the nuclei number in the sol solution also increased [12]. In addition, when the Al amount reduced, the geometric structure of the crystallites looked flat. Besides, the densities of the RTA samples were higher than those of the TF samples due to the rapid heating process [12]. In contrast, the surface roughness was relatively large (Figure 3c ~ 3f) due to the slow growth rate of the TF process.

From Figures 3g ~ 3j, we can see that the situation of the RTA process is similar to that of the TF process. With a certain amount of Mg, the crystallite size became smaller as the Al percentage increased due to the increasing number of the nuclei. However, there were small pores between the grains. Unlike that of the TF process, the geometric structure of the crystallites of the RTA process was all granular. The surface of the AMZO films was not very rough due to the fast growth procedure. To sum up, the morphology of films obtained from the RTA process is finer and evener than that from the TF process. Compared with the AZO films in our earlier studies [8], the morphology of the AMZO films obtained in this study shows no obvious differences.

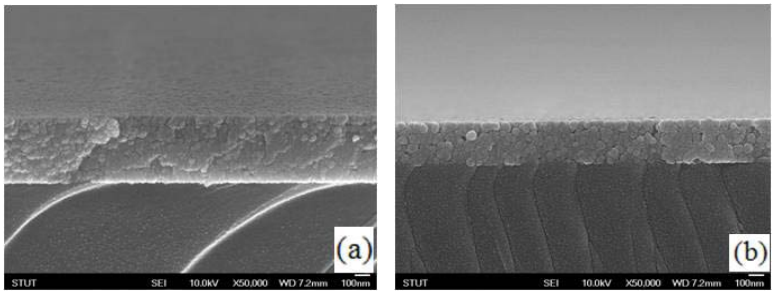

(a) RTA-AMZO, 0.5 % Mg – 0.75 % Al, 15-layers; (b) RTA-AMZO, 0.5 % Mg – 0.75 % Al, 8-layers;

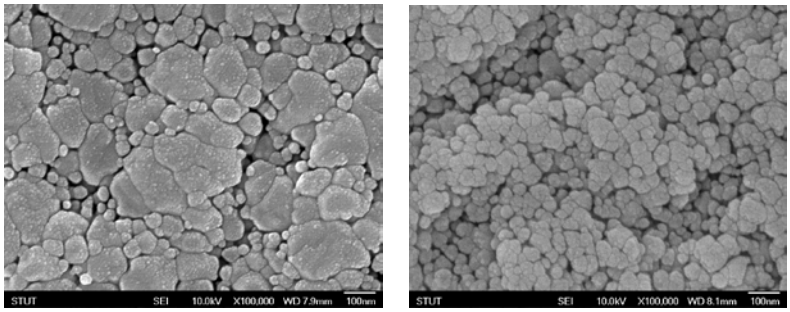

(c) TF-AMZO, 0.5 % Mg – 0.25 % Al; (d) TF-AMZO, 0.5 % Mg – 0.5 % Al;

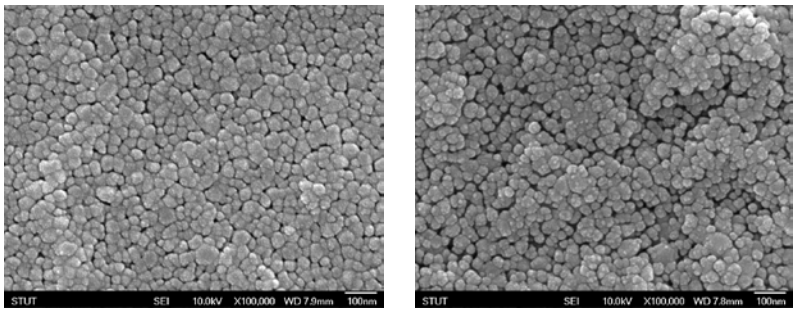

(e) TF-AMZO, 0.5 % Mg – 0.75 % Al; (f) TF-AMZO, 0.5 % Mg – 1.0 % Al;

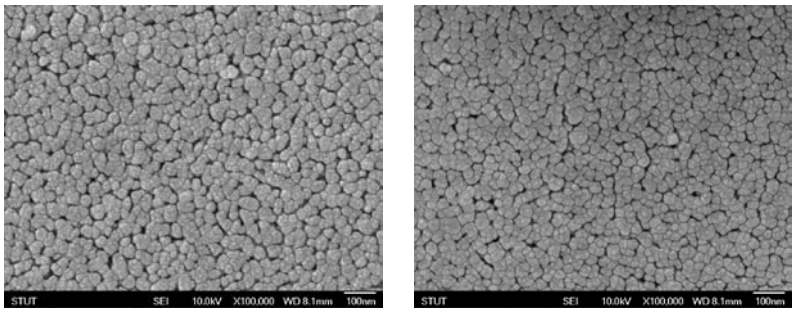

(g) RTA-AMZO, 0.5 % Mg – 0.25 % Al; (h) RTA-AMZO, 0.5 % Mg – 0.5 % Al;

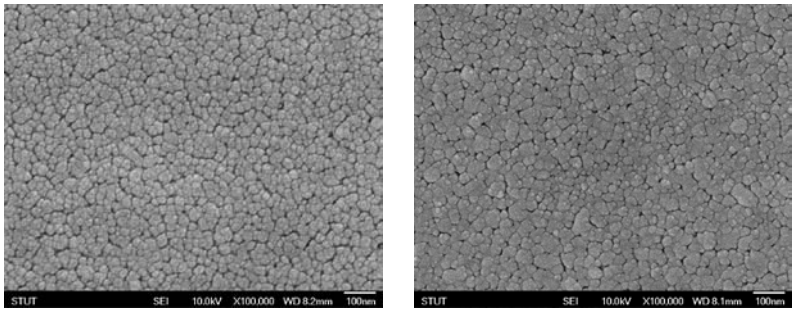

(i) RTA-AMZO, 0.5 % Mg – 0.75 % Al; (j) RTA-AMZO, 0.5 % Mg – 1.0 % Al.

Figure 3 Top view and cross-sectional SEM images of RTA- and TF-samples.

3. Analyses of Electrical Properties

The results of the Hall measurements are described in Figure 4 ~ 8. For the RTA process (Figure 4), when the amount of the dopants was small (≤ 0.5 at.%), the carrier concentration was obviously lower although the carrier mobility could reach 20 cm^2/Vs. As a result, the conductivity was low. On the other hand, when the doping amount was > 1.0 at.%, the carrier concentration did not increase while the carrier mobility dropped to around 15 cm^2/Vs. Consequently, the resistivity increased again. In general, when the doping ratio was 0.5 ~ 1.0 at.%, not only the carrier concentration was higher, but the mobility was also better. Thus, the resistivity of the AZO films was the lowest in this range. Compared with the results of our earlier studies [9], the electrical properties of the AZO films were improved in a similar way, i.e., the improvement of the AZO films' conductivity is the increase of the carrier concentration.

When the AZO films were co-doped with 0.5 or 1.0 at.% Mg, the carrier concentration rose slightly along with the increasing Al% amount (Figure 5). When Al% was higher than 0.75 at.% and reached 1.0 at.%, the carrier concentration dropped again while the mobility also dropped as Mg% increased (Figure 6). When Mg was 0.5 at.% and Al was 0.75 at.%, the conductivity of the AMZO thin films was slightly better ($2.66\times10^{-3}\Omega$cm) than that of the best AZO film ($3.17\times10^{-3}\Omega$cm) (Figure 7).

In the TF processes (Figure 8), the AMZO samples also had lower average resistivity ($9.01\times10^{-3}\Omega$cm) than the AZO ones (ca. $1.0\times10^{-2}\Omega$cm) when Mg was 0.5 at.% and Al was 0.5 at.%. However, their electrical properties were far worse than those of the RTA samples and were similar to the electrical properties of the TF samples in our earlier studies [8], suggesting that MgAc did not improve the activation of Al dopant during the TF process.

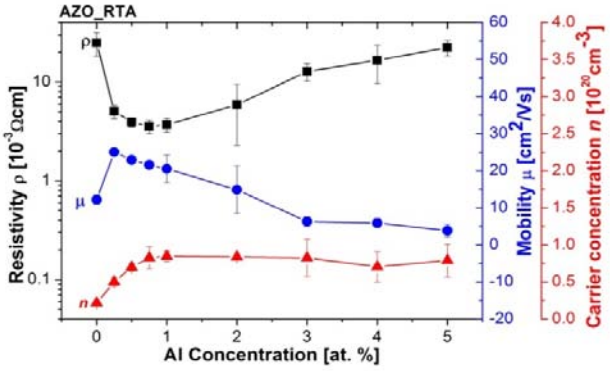

Figure 4 Hall measurements of the RTA-AZO films.

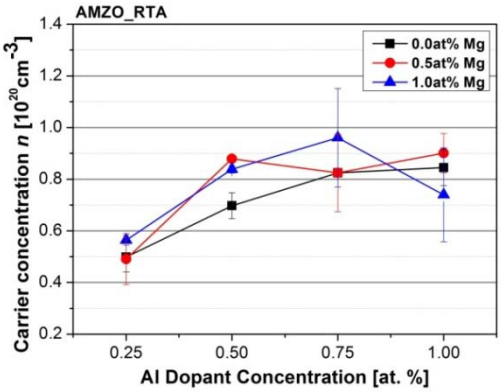

Figure 5 Carrier concentration of the RTA-AMZO films.

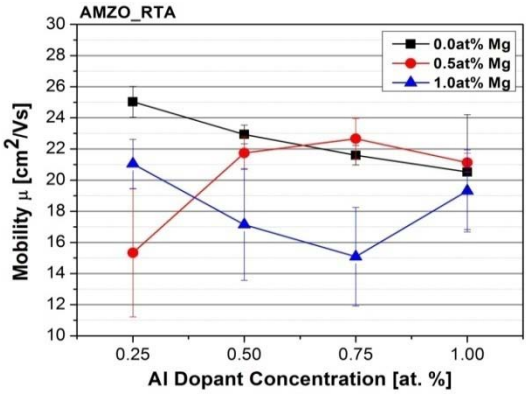

Figure 6 Carrier mobility of the RTA-AMZO films.

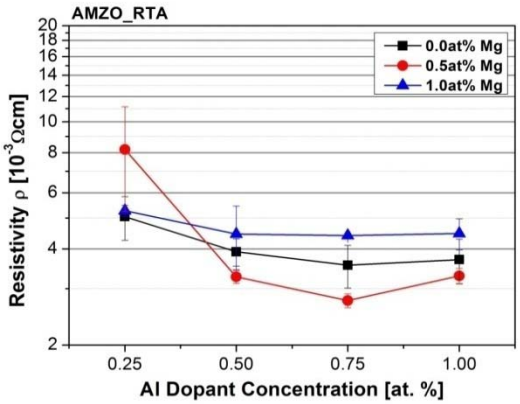

Figure 7 Electrical resistivity of the RTA-AMZO films.

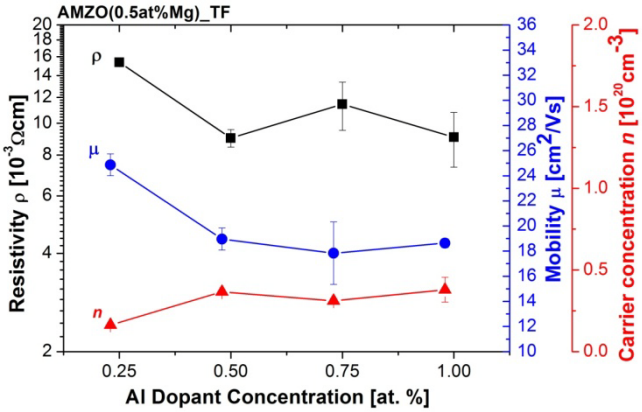

Figure 8 Hall measurements of the TF-AMZO films.

4. XPS and XRD analyses

From XPS analyses we found that the V_O-like bond of the TF-AZO specimens concentrated on the upper parts of the thin films (Figure 9). The V_O-like bonds suggest the oxygen vacancies within the ZnO matrix or within the amorphous ZnO, or it even could be the Ga-O or Al-O bonds [9]. In the RTA processes, although the

values of some points were not very high, but at least there were no continuous regions with the value of zero, like those of the TF specimens. This proved that co-doping Mg could further enable the Vo-like bonds to distribute more evenly in the RTA process whereas the Vo-like bonds still concentrated in the upper parts of the TF specimens even though Mg was added. Because Mg is more electropositive than Al, it was easy for Mg to form oxides during the slow crystallization process and segregated into the grain boundary of ZnO crystallites. Thus, Mg did not affect the following activation process.

The XRD patterns of some RTA-AZO, RTA-AMZO and TF-AMZO samples are plotted in Figure 10. From the figure, we found that adding Mg did not change the microstructure, i.e., the preferred orientation, of the RTA films. But the preferred orientation of AMZO films obtained from the TF process is obviously different from that of RTA samples. But the microstructure of AMZO films obtained from the TF process is obviously different from that of RTA samples. This also agrees with the discussion above, i.e., different film growth behaviors result in different distributions of dopants and diverse activation effects.

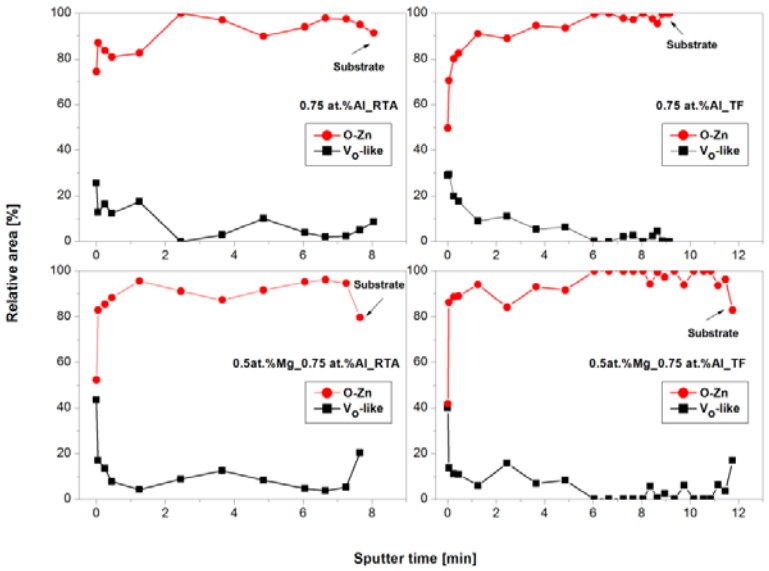

Figure 9 XPS depth profiles of AZO and AMZO samples.

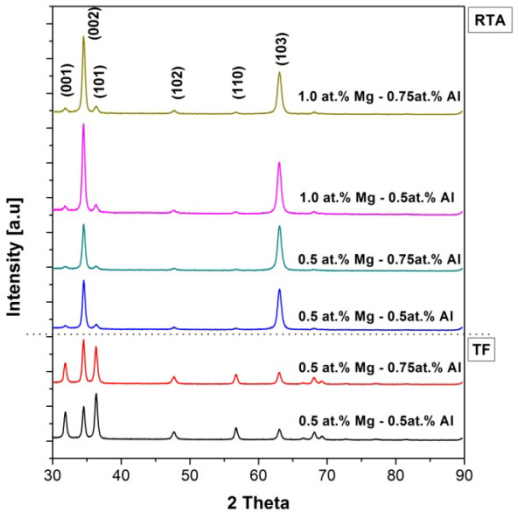

Figure 10 XRD patterns of RTA-AZO, RTA-AMZO and TF-AMZO samples.

IV. Conclusions

From the experimental results, we can conclude that the RTA process can effectively increase the activation and conductivity of AZO films. These results agree well with those of our earlier studies [9]. In addition, using Mg as co-dopant could slow the precipitation of ZnAc and retard the oxidization of Al. Thus, a proper amount of Mg can improve the conductivity of the AZO films. Consequently, under the prerequisite of using eco-friendly stabilizer, to enhance the carrier concentration by evenly distributing the dopant on the ZnO matrix to avoid the segregation of dopant materials on the grain boundary is more effective than by improving the film quality, i.e., improving the carrier mobility. Using amorphous films is one possible solution for this problem. Such a solution is being studied.

References

[1] A. G. Aberle, Thin-film solar cells, *Thin Solid Films* 517 (2009) 4706–4710.

[2] S. Calnan, A.N. Tiwari, High mobility transparent conducting oxides for thin film solar cells, *Thin Solid Films* 518 (2010) 1839–1849.

[3] S. Major, S. Kumar, M. Bhatnagar & K.L. Chopra, Effect of hydrogen plasma treatment on transparent conducting oxides, *Appl. Phys. Lett.* 49 (1986) 394–396.

[4] N. F. Cooray, K. Kushiya, A. Fujimaki et al., Large area ZnO films optimized for graded band-gap Cu(InGa)Se_2-based thin-film mini-modules, *Sol. Energy Mater. Sol. Cells* 49 (1997) 291–297.

[5] N. G. Dhere, Present status and future prospects of CIGSS thin film solar cells, *Sol. Energy Mater. Sol. Cells* 90 (2006) 2181–2190.

[6] T. Minami, Present status of transparent conducting oxide thin-film development for Indium-Tin-Oxide (ITO) substitutes, *Thin Solid Films* 515 (2008) 5822–5828.

[7] S. Suzuki, T. Miyata, M. Ishii & T. Minami, Transparent conducting V-co-doped AZO thin films prepared by magnetron sputtering, *Thin Solid Films* 434 (2003) 14–19.

[8] K. Lin, Y. Y. Chen & K. Y. Chou, Solution derived Al-doped zinc oxide films: doping effect, microstructure and electrical property *J. Sol-gel Sci. Techn.* 49 (2009) 238–242.

[9] K. Lin, Y. Y. Chen & C. Y. Chiu, Effects of growth behaviors on chemical and physical properties of sol–gel derived ZnO:Ga films, *Sol-gel Sci. Techn.* 55 (2010) 299–305.

[10] A. E. J. Gonzalez, J. A. Soto Urueta, R. Suarez-Parra, Optical and electrical characteristics of aluminum-doped ZnO thin films prepared by sol-gel technique, J. *Cryst. Growth* 192 (1998) 430–438.

[11] S. Bandyopadhyay, G. K. Paul, R. Roy, S. K. Sen and S. Sen. Study of structural and electrical properties of grain-boundary modified ZnO films prepared by sol–gel technique, *Mater. Chem. Phys.* 74 (2002) 83–91.

[12] I. V. Markov, Crystal Growth for Beginners: Fundamentals of Nucleation, Crystal Growth and Epitaxy, *World Scientific* (2003).